Pis'ma v ZhETF, vol. 91, iss. 8, pp. 405 – 409 © 2010 April 25

Interference Effects in the Conical Emission of Femtosecond Filament in Fused Silica

A. E. Dormidonov[1)], *V. P. Kandidov*, *V. O. Kompanets*[+], *S. V. Chekalin*[+]

M.V. Lomonosov Moscow State University, Physics Department, 119991 Moscow, Russia

[+]*Institute of Spectroscopy RAS, 142190 Troitsk, Moscow Region, Russia*

Submitted 25 February 2010

It is shown both experimentally and theoretically that interference effects play the key role in the formation of frequency-angular spectrum of the filament conical emission. For the first time we investigated experimentally the transformation of the conical emission frequency-angular spectrum with increasing of the filament length inside fused silica. We discovered the appearance of fine structure of the conical emission rings produced by lengthy filament. It is shown that the conical emission frequency-angular spectrum is produced by interference of coherent radiation from one or several moving point sources in the filament. The shape of the conical emission spectrum depends on the medium material dispersion, the spectrum structure is determined by length and relative location of filament emitting regions.

Femtosecond laser pulse filamentation in transparent dielectrics is accompanied by the superbroadening of the pulse frequency-angular spectrum. Anti-Stokes components of the supercontinuum (SC) which propagate in the forward direction inside the thin cone surrounding the filament form a set of rainbow colored rings of the conical emission (CE). The formation of axial-symmetric colored rings is a fundamental feature of the pulse spectrum nonlinear-optical transformation in the process of filamentation. The ring-shaped picture of the CE doesn't reshape in the case of astigmatic beams [1], nor depends on the location of SC generation region along the filament length [2]. Splitting of the CE continuous pattern into discrete colored rings was registered in air after refocusing of femtosecond pulse in the filament [3], inside fused silica during the filamentation of laser pulse focused by the axicon [4], inside fused silica with increasing of pulse energy [5]. The coherence length of the SC spectral components is not shorter than the coherence of the pump laser pulse [6] so that in the multifilamentation process of high-power femtosecond pulses the interference of the CE rings occurs [7]. A regular interference picture of the CE was obtained in [8] where the one-dimensional array of filaments was formed in water by the cylindrical lens.

Different models have been proposed for interpretation of the SC CE in the filament: a Cerenkov-type process on the filament dynamical surface [1, 9], four-photon parametric generation in the Kerr medium with the normal group-velocity dispersion [10], inseparable self-phase modulation in space and time [2, 11], three-wave mixing of the incident laser field and material waves of the medium nonlinear response [12]. In [13, 14] the filamentation and the SC generation were interpreted as a spontaneous formation and the subsequent dynamical interaction of X-wave packets. The interference model of the CE frequency-angular spectrum formation was proposed in [15].

In this letter we present new experimental and theoretical results on the interference effects in the process of the CE frequency-angular spectrum formation. For the first time we discovered the appearance of fine structure in the CE spectrum with increasing of filament length inside a fused silica sample. It is shown that CE frequency-angular spectrum is the result of the interference of broadband radiation from moving point sources in the filament. We present analytical expressions for frequency-angular distribution of spectral intensity, which reveal a fine structure typical for the CE produced by lengthy filament and the CE ring splitting after refocusing. We show that in a medium with a normal group-velocity dispersion the CE results from the interference of the radiation outgoing from several subpulses moving with different velocities.

The experimental setup is shown schematically in the Fig.1. Ti:sapphire laser pulses (800 nm wavelength, 1 kHz repetition rate) with duration 35 fs and diameter 3 mm (FWHM) were focused by the 100-cm lens onto the sample input face. The original element of our setup was the sample, which represented an optically polished acute-angled wedge made of the fused silica UV-1. The wedge had 10-cm height and 4-cm width. In front of the silica wedge as well as behind it there was no filamentation, because the pulse peak power was of three

[1)] e-mail: dormidonov@gmail.com

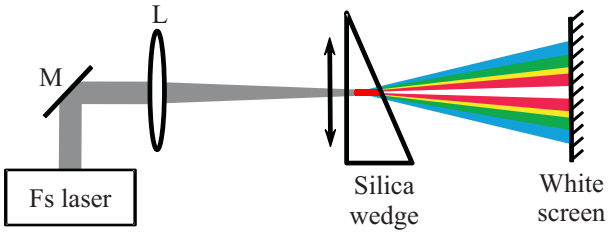

Fig.1. Schematic representation of our experimental setup for the registration of the SC CE from filament with varied length

orders less than the critical power for self-focusing in air. The wedge was mounted on the translation stage with the possibility of the micrometer resolution movement in the plane perpendicular to the beam propagation direction. Such arrangement enabled slow variation of the filament length inside the sample and therefore make it possible to investigate the CE spectrum transformation from filament start and till multiple refocusings at the same pulse energy. The length, location, and structure of glowing filament inside a silica were registered by the digital camera with the microscope objective through the side face of the wedge. The SC CE was observed and recorded by another digital camera on the white screen placed at the distance of 20 cm from the wedge input face.

For the investigation of the SC CE frequency-angular spectrum we fixed the laser pulse energy on the value of $2.4\,\mu$J that corresponds to the pulse peak power of about $30P_{cr}$, where P_{cr} – the critical power for self-focusing in fused silica. For such energy parameters several refocusings can occur in a lengthy sample. The starting point of the filament takes place at the distance $z_f = 6.5$ mm from the input face of the wedge. When the wedge was fitted in position where laser pulse passed inside it the distance equaled to the z_f and then get out from the silica sample, we observed only the glowing point near the output face of the wedge (Fig.2a). Therefore, it becomes possible to observe CE formed by the point SC source in the filament. In this case CE represents a wide homogeneous red spot (Fig.3a). This indicates the beginning of the frequency-angular spectrum broadening. When slowly moving the wedge upward in order to increase the laser pulse passing distance inside the nonlinear medium the longer filament is formed. When the filament length l, which is limited by the wedge, is about 1 mm (Fig.2b) the CE represents a white spot surrounded by a blue aureole. This is the evidence of the considerable broadening of frequency-angular spectrum and increasing of the anti-Stokes components intensity. Further growing of the filament length results in the CE higher brightness. At the filament length $l = 2$ mm (Fig.2c) characteristic continuous rainbow colored rings appear in the CE pattern extending from red (longer wavelength) near the center to blue (shorter wavelength) at the outside (Fig.3c). When the filament length l exceeded 2.5 mm (Fig.2d) we discovered the appearance of a fine structure in the angular distribution of the rainbow rings (Fig.3d) (compare with Fig.3c). The angular width of the discrete rings forming the fine structure is about 0.003 rad and decreases with the filament length growing. The discovered fine structure of the CE rings can be explained by formation of interference maxima in the frequency-angular spectrum generated by a lengthy filament.

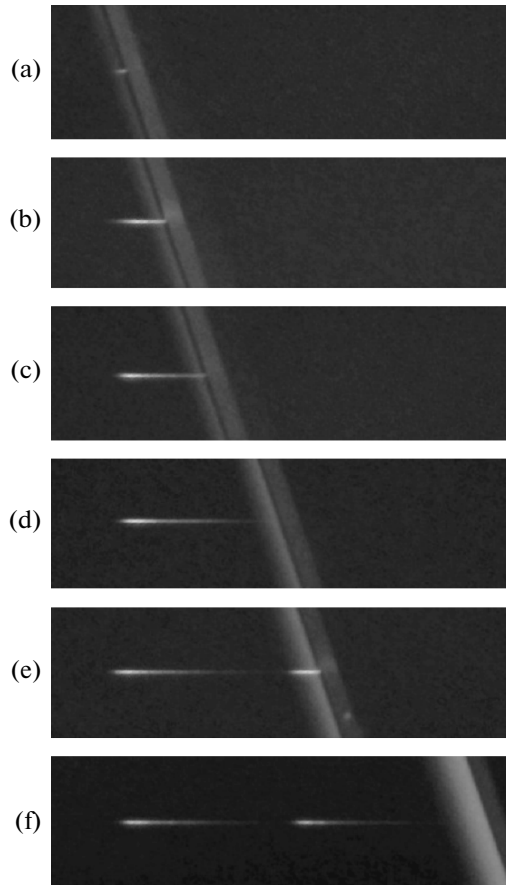

Fig.2. Images of the filament inside the silica wedge at different wedge positions. The inclined light line is the output face of the wedge

Subsequent wedge shifting leads to the attainment of the sufficient pass distance of the laser pulse inside the silica for the refocusing. At the distance $L \approx 2.7$ mm after the starting point of the filament the refocusing occurs, and the second emitting region in the filament begin to appear coaxially with the first one (Fig.2e). The appearance of the second emitting region leads to the splitting of the CE pattern into the discrete high-

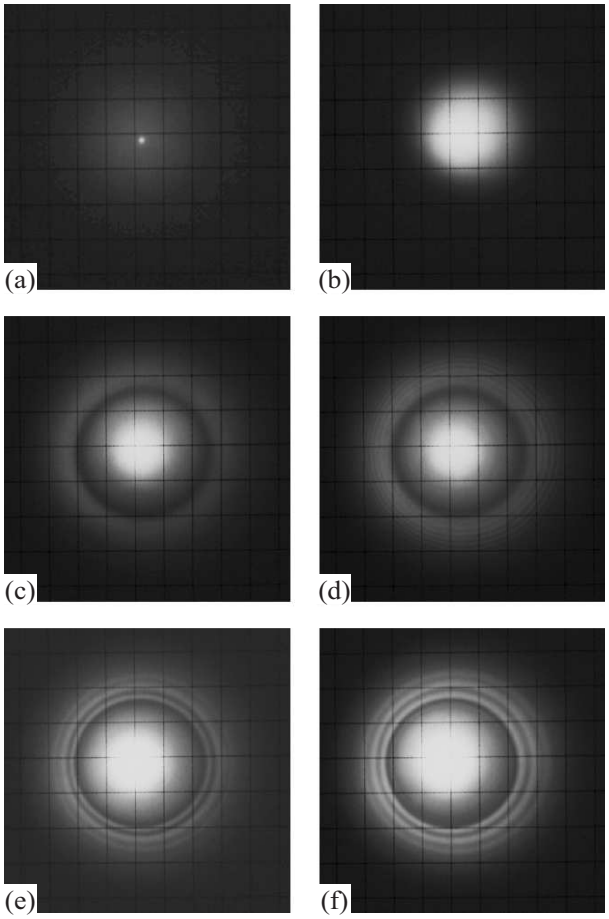

Fig.3. Patterns of the conical emission corresponding to different filament lengths from the Fig.2. Pulse parameters: wavelength 800 nm, duration 35 fs (FWHM), energy 2.4 μJ

contrast colored rings of the 0.005 rad angular width (Fig.3e). With the growth of the second emitting region length (Fig.2f) the discrete rings of the CE become more brightly and contrasting, but its angular width doesn't change (Fig.3f).

The analysis of the obtained experimental results leads to the conclusion that the SC CE is formed by the interference of light fields from one or several lengthy emitting regions of the filament. Angular distribution of the SC CE depends on the length and the relative position of emitting regions in filament.

For theoretical explanation of the appearance of the fine structure in the CE angular spectrum with the filament length increasing and also of the colored rings splitting after refocusing we used our interference model [15]. According to the model, the CE frequency-angular spectrum is formed as a result of the interference of the point broadband source radiation, which moves with the group velocity v_g along the emitting filament region. In this case the frequency-angular distribution of the spectral components $S(\theta,\lambda)$ takes the form:

$$S(\theta,\lambda) = S_0(\theta,\lambda) l^2 \mathrm{sinc}^2\left(\frac{\Delta\varphi(\theta,\lambda)}{2}\right), \qquad (1)$$

where l is the length of the filament emitting region, $S_0(\theta,\lambda)$ is the spectrum of the point source. The phase shift $\Delta\varphi(\theta,\lambda)$ of the CE component at the wavelength λ propagating under the angle θ is equal:

$$\Delta\varphi(\theta,\lambda) = \frac{2\pi l}{\lambda_0}\left(\left(1-\frac{\lambda_0}{\lambda}\right)\frac{c_0}{v_g} - \left(1-\frac{\lambda_0 n(\lambda)}{\lambda n_0}\cos(\theta)\right) n_0\right), \qquad (2)$$

where λ_0 is the pulse central wavelength, $n_0 = n(\lambda_0)$. The refractive index $n(\lambda)$ and the group velocity v_g are calculated from the dispersion relation for the medium.

The CE spectrum formed by the interference of the radiation from two filament emitting regions in case of the refocusing is calculated from the following analytical expression [5, 15]:

$$S_\Sigma(\theta,\lambda) = 4S(\theta,\lambda)\cos^2\left(\frac{\Delta\varphi_\Sigma(\theta,\lambda)}{2}\right), \qquad (3)$$

where $S(\theta,\lambda)$ is the spectral intensity of the conical emission, formed by each of the separate emitting regions with the length l. Spectral intensity $S(\theta,\lambda)$ can be calculated analytically from eq. (1). The phase shift $\Delta\varphi_\Sigma(\theta,\lambda)$ for the waves from different emitting regions of the filament is calculated from eq. (2) by the substituting l for the distance L between the starting points of the emitting regions.

In the filamentation process occurring inside the Kerr medium with the normal group-velocity dispersion a laser pulse splits into two subpulses. Each subpulse represents the SC source, which propagates inside the medium with its own velocity, different from the pulse group velocity v_g due to the different subpulse spectral contents. In this case the analytical expression for the angular distribution of the CE spectral components $S(\theta,\lambda)$ can be also obtained from the interference model [15]:

$$S(\theta,\lambda) = \left|\sqrt{S_{01}(\theta,\lambda)} l_1 \mathrm{sinc}\left(\frac{\Delta\varphi_1(\theta,\lambda)}{2}\right) e^{i\frac{\Delta\varphi_1(\theta,\lambda)}{2}} + \sqrt{S_{02}(\theta,\lambda)} l_2 \mathrm{sinc}\left(\frac{\Delta\varphi_2(\theta,\lambda)}{2}\right) e^{i\frac{\Delta\varphi_2(\theta,\lambda)}{2}}\right|^2. \qquad (4)$$

Here $S_{01,2}(\theta,\lambda)$ are the spectrum intensities of each SC point source, $\Delta\varphi_{1,2}(\theta,\lambda)$ are calculated from eq. (2) assuming $l = l_{1,2}$ and $v_g = v_{1,2}$, respectively, $l_{1,2}$ are the sources emitting lengths, $v_{1,2}$ – sources velocities.

The "visible" spectrum $S_h(\theta,\lambda) = S(\theta,\lambda)h(\lambda)$ corresponds to the broadband spectrum perceptible by the human eye, where $h(\lambda)$ is the spectral sensitivity of the digital camera used to record the CE patterns.

Figs. 4a,d present the "visible" CE spectra $S_h^{an}(\theta,\lambda)$ calculated analytically by (1)–(4) for experiment parameters. Fig.4a corresponds to the CE spectrum from

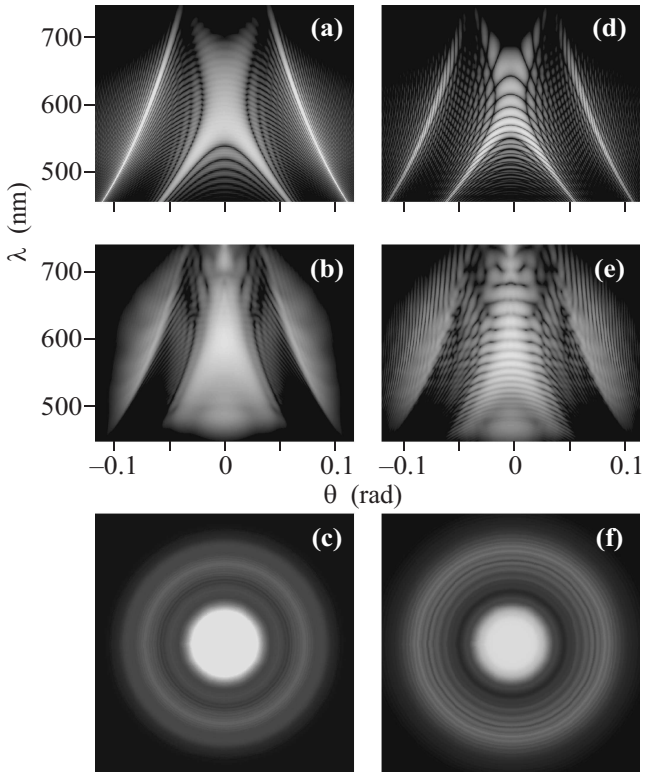

Fig.4. a),d) – halftone pictures of the "visible" analytical CE frequency-angular spectra $S_h^{an}(\theta,\lambda)$ for a) one emitting region with the length $l = 2.5$ mm and d) two filament emitting regions with the distance between its starting points $L = 2.7$ mm. b), e) – numerical CE frequency-angular spectra $S_h^{sim}(\theta,\lambda)$ at the distances b) $z = 9.5$ mm (before the refocusing) and e) $z = 12.5$ mm (after the refocusing). c), f) – corresponding CE ring patterns, which are reconstructed from numerical spectra $S_h^{sim}(\theta,\lambda)$ in format of the experiment. Pulse parameters are the same as in experiment

the one emitting region with the length $l = 2.5$ mm, Fig.4d – from the two filament emitting regions with the distance between its starting points $L = 2.7$ mm. Emitting regions are formed by two subpulses. In the Fig.4a the angular distribution of the "red" spectral component ($600 \div 730$ nm) contains several side maxima corresponding to the thin red discrete rings of the CE fine structure discovered in the experiment (Fig.3d). Appearance of side maxima is explained by the interference of light field from the lengthy emitting region of filament (Fig.2d). The angular width (0.0025 rad) and locations (0.05 rad) of the interference maxima in the spectrum $S_h^{an}(\theta,\lambda)$ are in good agreement with the experimental results. In the CE spectrum from the two filament emitting regions, which formed after refocusing (Fig.2e,f), the high-contrast modulation of the spectral intensity appears over the angle θ and the wavelength λ (Fig.4d). This modulation is independent from the length l_2 of the second emitting region. The pronounced angular modulation in the wavelength band $600 \div 730$ nm reproduces the splitting of the CE pattern into the high-contrast discrete colored rings observed in the experiment (Fig.3e,f). It have to be noted that zero order maxima in the distribution $S_h^{an}(\theta,\lambda)$ of interference model coincide with areas of the effective transfer of the laser pulse energy, which were obtained in [12] from the phase-matching condition for tree wave mixing. However the model [12] doesn't reproduce the fine structure of the CE spectrum.

We also performed computer simulations of the frequency-angular spectrum broadening in the filamentation of femtosecond laser pulses in fused silica. The mathematical model [15] of the filamentation takes into account the diffraction and the nonlinear-optical interaction of the femtosecond laser radiation with the medium as well as the full material dispersion by means of Sellmeier formula.

Figs.4b,e show the numerical "visible" frequency-angular spectra $S_h^{sim}(\theta,\lambda)$ of the laser pulse with the energy $2.4\,\mu$J obtained from the computer simulations for different distances z. Ring patterns of the CE reconstructed in format of experiment from numerical spectra $S_h^{sim}(\theta,\lambda)$ are shown in Figs. 4c,f. At the distance $z = 9.5$ mm, when the filament length l is about 2.5 mm (filament start $z_f = 7.0$ mm), the angular modulation appear in the frequency-angular distribution $S_h^{sim}(\theta,\lambda)$ in the vicinity of $\theta = 0.05$ rad (Fig.4b). This modulation corresponds to the thin rings of the CE (Fig.4c), which were observed in the experiment (Fig.3d) and coincides with the side maxima of the analytical spectrum $S_h^{an}(\theta,\lambda)$ (Fig.4a). As follows from the numerical simulation at the distance $z \approx 10$ mm the refocusing occurs ($L = 3$ mm), that is in good agreement with the experiment (Fig.2e). High-contrast modulation in the numerical spectrum $S_h^{sim}(\theta,\lambda)$ (Fig.4e) and reconstructed rings pattern (Fig.4f) are in good agreement with modulation in the analytical spectrum $S_h^{an}(\theta,\lambda)$ (Fig.4d) and experimental discrete rings (Fig.3e,f), respectively.

We investigated experimentally, analytically, and numerically the interference effects in the course of supercontinuum CE generation in fused silica. The fine structure of the CE colored rings was discovered with increasing of filament length. Refocusing and appearance of the second emitting region in the filament leads to splitting of the CE rings into the high-contrast discrete colored rings. We proposed the interference model according to which the CE frequency-angular spectrum is the result of the interference of broadband radiation from moving point sources in the filament. In a medium with normal group-velocity dispersion after pulse splitting into subpulses the CE results from the interference of radiation outgoing from several point sources moving with different velocities. The CE fine structure and ring splitting is explained by interference of coherent waves from one or, respectively, several lengthy emitting regions of the filament. Taken into account the pulse splitting in the interference model leads to the good correlation with the numerical simulation and the laboratory experiment.

This work was supported by the Russian Foundation for Basic Research (Grant # 08-02-00517-a) and by the Russian Federal Agency for Science and Innovation (Rosnauka, the state contract 02.740.11.0223).

1. I. Golub, Opt. Lett. **15**, 305 (1990).
2. O. G. Kosareva, V. P. Kandidov, A. Brodeur et al., Opt. Lett. **22**, 1332 (1997).
3. S. L. Chin, S. A. Hosseini, W. Liu et al., Canadian J. of Phys. **83**, 863 (2005).
4. O. G. Kosareva, A. V. Grigor'evskii, and V. P. Kandidov, Quantum Electronics **35**, 1013 (2005).
5. A. E. Dormidonov, V. P. Kandidov, V. O. Kompanets, and S. V. Chekalin, Quantum Electronics **39**, 653 (2009).
6. S. L. Chin, A. Brodeur, S. Petit et al., J. of Nonlinear Opt. Physics and Materials **8**, 121 (1999).
7. W. Liu, S. A. Hosseini, Q. Luo, B. Ferland et al., New Journal of Physics **6** (2004).
8. K. Cook, A. K. Kar, and R. A. Lamb, Appl. Phys. Lett. **83**, 3861 (2003).
9. E. T. J. Nibbering, P. F. Curley, G. Grillon et al., Opt. Lett. **21**, 62 (1996).
10. G. G. Luther, A. C. Newell, J. V. Moloney, and E. M. Wright, Opt. Lett. **19**, 789 (1994).
11. V. P. Kandidov, O. G. Kosareva, I. S. Golubtsov et al., Appl. Phys. B **77**, 149 (2003).
12. M. Kolesik, E. M. Wright, and J. V. Moloney, Optics Express **13**, 10729 (2005).
13. C. Conti, S. Trillo, P. Di Trapani et al., Phys. Rev. Lett. **90**, 170406 (2003).
14. D. Faccio, A. Couairon, and P. D. Trapani, *Conical Waves, Filaments and Nonlinear Filamentation Optics*, ARACNE, Rome, 2007, p. 162.
15. A. E. Dormidonov and V. P. Kandidov, Laser Physics **19**, 1993 (2009).